LAND CLASSIFICATION OF WAVELET-COMPRESSED FULL-WAVEFORM LIDAR DATA

S. Laky [a,b], P. Zaletnyik [a,b], C. Toth [b]

[a] Budapest University of Technology and Economics, HAS-BME Research Group for Physical Geodesy and Geodynamics, Muegyetem rkp. 3. Kmf. 16., Budapest, H-1111, Hungary, zaletnyikp@gmail.com, laky.sandor@freemail.hu
[b] The Ohio State University, The Center for Mapping, 470 Hitchcock Hall, 2070 Neil Avenue, Columbus, OH 43210, United States, toth@cfm.ohio-state.edu

Commission III, WG III/2

KEY WORDS: LiDAR, full-waveform, surface classification, wavelet compression

ABSTRACT:

Given sufficient data storage capacity, today's full-waveform LiDAR systems are able to record and store the entire laser pulse echo signal. This provides the possibility of further analyzing the physical characteristics of the reflecting objects. However the size of the captured data is enormous and currently not practical. Thus arises the need for compressing the waveform data. We have developed a methodology to efficiently compress waveform signals using a lossy compression technique based on the discrete wavelet transform. Land classification itself is also a non-trivial task. We have implemented an unsupervised land classification algorithm, requiring only waveform data (no navigation data is needed). For the classification Kohonen's Self-Organizing Map (SOM) has been used. Finally, the effect of the information loss caused by the lossy compression scheme on the quality of the land classification is studied.

1 INTRODUCTION

Airborne laser scanning (airborne LiDAR or ALS) is used in many areas: digital elevation model generation, city modeling, forest parameters estimation, etc (Shan and Toth, 2009).

During the development of the ALS systems, first only one backscattered echo per emitted pulse was provided to the user. Later the first and the last echoes became available. Multi-echo or multiple pulse laser scanning systems are able to measure up to six pulses. The newest generation of ALS systems, the full-waveform systems, are able to digitize and record the entire backscattered signal of the emitted pulses (Mallet and Bretar, 2009).

This technology provides the possibility of further analyzing the physical characteristics of the reflecting objects (Jutzi and Stilla, 2005, Wagner et al., 2004). Adding sufficient data storage capabilities to the system, the waveform data can be easily made available to users, thus the derived end products can be improved by analyzing the waveform data. However, this raises two questions.

The first is the question of data storage and transfer. Currently, the needed storage space is huge. For example, during a test flight above Toronto (Ontario, Canada) 60 seconds of full-waveform data has been collected. This means approximately 4,000,000 waveforms, needing 580 Mbytes of additional storage space to the original 460 Mbytes sensor navigation data (GPS time, latitude, longitude, elevation, pitch, roll, heading, etc.). It can easily be calculated, that for a 3-hour-long flight more than 180 Gbyte of storage space is needed. Thus the need for compressing the raw waveform data arises. Our primary goal is to develop a compression method which, if it is implemented in real-time in the software layer of the waveform digitizer unit, is able to reduce the needed data storage capacity, thus extend the acquisition time. Moreover organizations who store large amount of archived data can also benefit from such a compression scheme. In this study, we use a lossy approach to the data compression (Sayood, 2006). Our method is based on the CDF (Cohen-Daubechies-Feauveau) 3/9 wavelet transform (Cohen et al., 1992) of the waveform, and

a linear quantization algorithm with thresholding (Laky et al., 2010). This question is discussed in Section 2.

The second is the question of classification. As the first airborne laser scanners provided only 3D point clouds, the early algorithms used only LiDAR derived point clouds, based on the relative position of the points with respect to their neighbors. Later the recorded intensity values were also used. The full-waveform systems made it possible to extract more information from the backscattered signal. The most widespread is the use of Gaussian (Wagner et al., 2006) or Generalized Gaussian functions (Chauve et al., 2007) for representing the echos in waveforms, thus providing various parameters of it. The parameters of the modeling functions can be used also for classification purposes.

In this study, we use the moments and the maximum intensity of the waveform signal as input for an unsupervised classification with Kohonen's Self-Organizing Map (SOM (Kohonen, 1990)) (Zaletnyik et al., 2010). This question is further discussed in Section 3.

The combination of the two above techniques raises a third question: how the lossy nature of the wavelet-based compression influences the precision of the classification. This is discussed in Section 4.

2 WAVELET-BASED WAVEFORM COMPRESSION

2.1 Short introduction to the wavelet compression

Data compression methods, in general, can be divided into two main groups: lossless and lossy compression. Lossless compression algorithms, like run length encoding (RLE), Huffman coding or arithmetic coding, provide an exact reconstruction of the compressed data, with a limited compression rate. Lossy compression schemes, like transform coding schemes, provide the user the opportunity to choose between better reconstruction quality or better compression rate. Today's most widely known compression techniques (e.g. JPEG, MP3) are based on lossy compression methods utilizing Fourier or Fourier-related techniques.

Recently methods utilizing the discrete wavelet transform (DWT) have been developed (e.g. JPEG2000).

The principle of DWT-based compression is the following: we are looking for a base, in which the data to be compressed has a sparse or nearly sparse representation. This means, that the wavelet coefficient vector of the data (in this case the waveform signal) has many zero or near-to-zero elements (see Figure 1). After eliminating the elements having the lowest values (i.e. thresholding), we can store the coefficient vector in a more compact form.

(a) Typical waveform

(b) CDF/3/9 wavelet coefficients

First 25% of the wavelet coefficients (by order)

(c) Sorted magnitude of wavelet coefficients

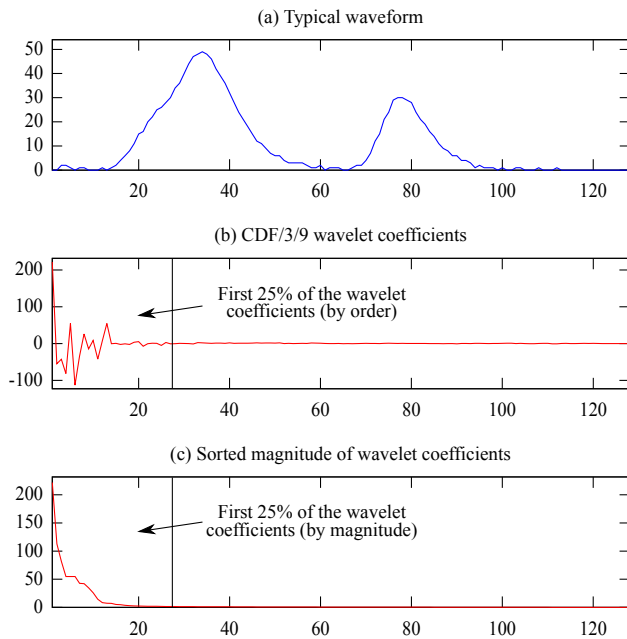First 25% of the wavelet coefficients (by magnitude)

Figure 1: CDF 3/9 wavelet transform of a typical waveform

The next key step of the compression algorithm is storing the remaining coefficients. In most cases, the wavelet coefficients are real numbers, even if the input signal is a discrete-valued one. In our case, the waveform signal has discrete values between 0 and 255. These values can be stored as 8-bit (1-byte) unsigned integers. The wavelet coefficients, however, are calculated as single precision (32 bits, 4 bytes) or double precision (64 bits, 8 bytes) floating point numbers. This offers great precision for storing the coefficients, but considerably increases the needed storage space. One solution to overcome this problem is to quantize the coefficients, i.e. to map the coefficients to certain discrete numbers, giving the opportunity to store these using a smaller number of bits.

The elimination of the not-exactly-zero elements and the quantization of the remaining coefficients cause the error of the reconstruction. The reconstruction quality is thus greatly influenced by choosing the wavelet family, the threshold, and the method and granularity of the quantization.

2.2 Applied compression method

For developing our compression method, we have been using the WaveLab toolbox (Buckheit and Donoho, 1995). The first task was to choose the best wavelet family for this purpose (Laky et al., 2010). The evaluation of the performance was based on the values of the standard deviation and the maximum absolute error of the reconstruction at given compression rates. The experiments were run on a sample of 500 representative waveforms from the test area. This time no quantization has been used, and

the threshold was chosen so, that all but the largest given percent of the wavelet coefficients became zero (e.g. in Figure 1(c), in case of a 0.25 (25%) compression ratio, all wavelet coefficients after the 25% mark are to be zeroed out).

The target compression ratio is 0.20. (The compression ratio is the ratio of the storage space needed for the compressed data versus the storage space needed for the uncompressed data. The lower the number, the better the compression performance is.) The performance of a few wavelet families, based on our evaluation, is listed in Table 1. In this range the CDF (Cohen-Daubechies-Feauveau) wavelet family outperforms the other wavelet families in terms of the average standard deviation and maximum absolute error of the reconstruction (the reconstruction error is the difference of the original signal and the signal after DWT, coefficient vector truncation and inverse DWT).

Wavelet family	Std of the error	Maximum absolute error
Haar	1.14	3.88
Daubechies	0.46	1.44
Symmlet	0.44	1.39
CDF	0.40	1.29

Table 1: Evaluating the performance of some wavelet families at 0.20 compression rate (errors in intensity units)

After further evaluation of the CDF family (regarding its parameter values), the CDF 3/9 wavelet has been selected. It is important to mention, that CDF is a biorthogonal wavelet family, which means, that different base functions are used for the analysis and the synthesis of the signal (see Figure 2).
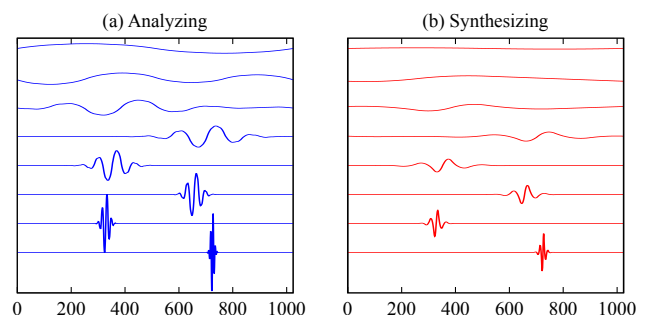

(a) Analyzing

(b) Synthesizing

Figure 2: CFD/3/9 wavelet base functions

The second parameter to choose was the quantization method of the wavelet coefficients. For this purpose, a 8-bit (256 levels) linear quantizer has been chosen. It is important to note, that the quantizer has to have a level for storing exactly zero values (i.e. it has to be a mid-tread quantizer). This is because of the nature of the wavelet compression.

Quantization threshold	Std of the error	Maximum absolute error	Compression rate
1.0	0.84	2.99	0.28
3.0	0.89	3.17	0.23
5.0	0.96	3.30	0.21
7.0	1.04	3.46	0.20
9.0	1.21	3.90	0.19

Table 2: Choosing the quantization threshold (errors in intensity units)

Finally the quantization threshold had to be chosen. The objective was to achieve the highest possible compression rate while not allowing the standard deviation of the reconstruction error to exceed 1.00 intensity values. After evaluating different choices,

a value of 5.0 has been decided (see Table 2). It is important to mention, that the choice of quantization threshold depends on the chosen wavelet family. Using wavelet families other than CDF may enable better compression rates than 0.21 using a threshold of 5.0, but the reconstruction quality may decrease (see Table 1).

The final scheme of the compression is the following:

1. Preparing the waveform signal for compression: the intensity values are decreased by 10.0 (this is the threshold value of the digitizer), and the signal is zero-padded at the end to have the length of the nearest power-of-two to the actual length (this is needed because WaveLab operates on signals of such length).

2. Calculating the CDF 3/9 wavelet transform of the waveform signal.

3. Truncating the coefficient vector at a length of 25% (see Figure 1(b)). This means, that only the average coefficients and the coefficients of first 4 detail level are kept. Our experiments have shown, that more than 99% of the signal energy is stored in the first 25% of the coefficients (see Figure 3).

4. The remaining coefficients are thresholded with a value of 5.0 (i.e. all the coefficients with a magnitude smaller than this value are made exactly zero).

5. The coefficients are quantized using a 8-bit (256-level) linear mid-thread quantizer. Actually only 255 levels are used for the quantization, the highest level is kept for special purposes (e.g. marking the end of the waveforms, or marking the blocks of the RLE compression in the next step).

6. An RLE compression is applied to the quantized coefficients, to find sequences of repeated values in the quantized coefficient vector (usually sequences of zeros are found), and replace them with shorter code blocks.
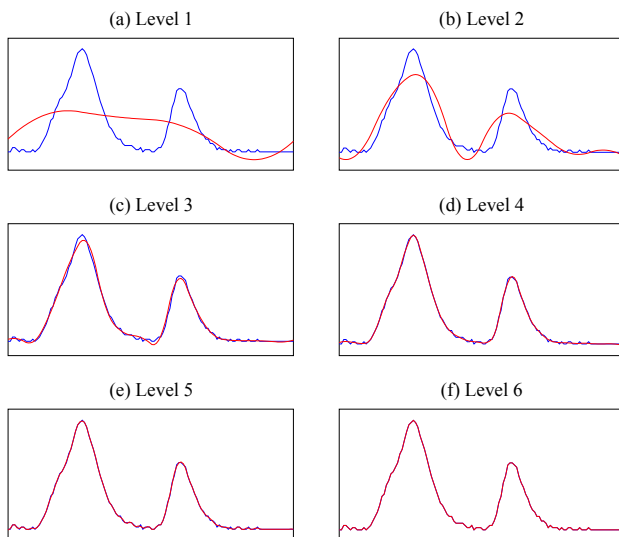

Figure 3: Reconstruction of a typical waveform using wavelet detail coefficients up to the specified levels

3 SOM-BASED CLASSIFICATION

As the recently appeared full-waveform LiDAR systems are able to digitize and record the entire backscattered signal, this provides the possibility of further analyzing the waveform and, thus, obtaining additional information about the reflecting object.

Many studies are dealing with LiDAR data classifications. The first LiDAR classification algorithms were based only on LiDAR derived geometric data (Maas, 1999), or were combined with other data acquisition method such as aerial imagery (Brattberg and Tolt, 2008). As now the entire waveform can be available to the users, the shape of the waveforms can be analyzed to derive more information. (Ducic et al., 2006) decomposed the waveforms into Gaussian components and used the parameters of the Gaussian functions, such as the maximum intensity and the standard deviation (pulse width) to separate vegetation and non-vegetation areas. (Mallet et al., 2008) used Generalized Gaussian model with one more parameter for classification purposes. Both studies used supervised classification algorithm.

Classification algorithms can be divided into two main groups, supervised and unsupervised classification. In the supervised classification a training and a test dataset is used, where we know the output class types belonging to the inputs. In the case of unsupervised classification, first data has to be grouped into clusters based on some measure of similarity. Then these groups can have classes associated with them (this can be done manually, or with the help of a small number of samples with known group-class correspondence). The advantage of this classification is that there is no need to have a priori knowledge of the class types belonging to a training or test dataset.

In this paper, the feasibility study of classifying the reflecting surface is based on Kohonen's Self-Organizing Map (SOM), an unsupervised learning algorithm. SOM was first described as an artificial neural network model by Teuvo Kohonen (Kohonen, 1990). Our choice is motivated by the flexibility of the algorithm (in terms of parametrization), and its ability to adopt well to highly non-linear mapping problems. The SOM_PAK program package, which was prepared by the SOM programming team of the Helsinki University of Technology (Kohonen et al., 1996) has been used.

The used sample LiDAR dataset is from Ontario, collected from a residential area of Scarborough (Toronto) by an Optech ALTM 3100 full-waveform LiDAR system. The original Scarborough area dataset contained more than 800 000 waveforms. For our classification study we have chosen a smaller area (50 x 65 m) containing different types of surface coverage (roof, pavement, grass, trees), with around 6000 waveforms. The distance between two adjacent points in a scan line is about 0.25 m, but the distance between the scan lines is about 2-3.5 m, which strongly influences the spatial resolution of the classified map.

In our approach the waveforms are first separated according to the number of peaks. For this we used a pulse detection method to count the number of the pulses in the waveforms. This basic peak detection method is based on the zero crossings of the first derivative on the thresholded version of the waveform (Chauve et al., 2007). In our method first we used a low pass filter to eliminate peaks caused by noise, and then the peaks were detected with the method referenced above.

After the waveforms were separated into two classes (one-echo and multiple-echo), the multiple-echo waveforms were classified as trees or roof. (Because multiple-echo waveforms can also appear due to other man-made objects, such as cars, etc., this causes some class speckle in the classification, which can later be removed by e.g. mode filtering.) The one-echo signals were treated as probability density functions, to determine important statistical parameters, according to the shapes of the waveforms, such as the maximum intensity value (amplitude), standard deviation (pulse width), skewness (measure of the asymmetry of the waveform,

third central moment) and the kurtosis (measure of the peakedness, fourth central moment). These parameters are then used as input parameters for the SOM algorithm. With this method grass, trees, pavement and roof can be separated quite well. The most problematic part is the separation between pavement and roof, where the slope has a very important role. In out case, one flat roof has been categorized as pavement. This problem can be solved applying a two step classification, using the local range differences in the second step. The ranges are calculated as the expected value of the probability density function plus the starting time of the backscattered waveform. In this way low areas (pavement) and locally high areas (roofs) can be separated well (Zaletnyik et al., 2010). The classification is based only on waveform data, i.e. no navigation data is used. This means, that the coordinates of the LiDAR points need not to be calculated to carry out the classification. Of course, the coordinates have to be calculated later to georeference the classified waveforms.
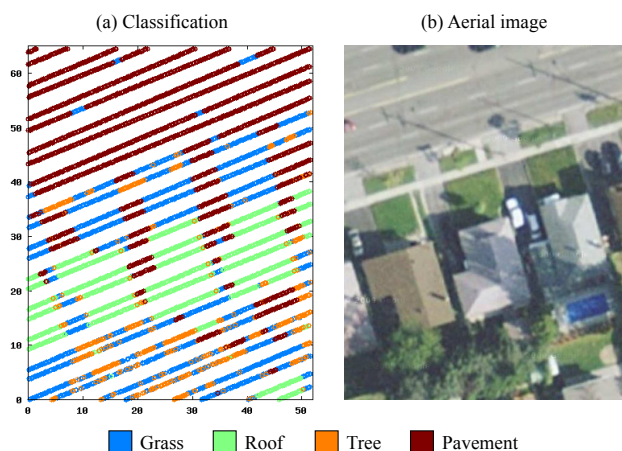

Figure 4: The result of the classification process. Aerial image: Google Maps.

The result of the classification is shown in Figure 4. Comparing the result with an aerial imagery visually, it can be seen that using the statistical parameters with unsupervised classification method, the waveforms can be classified effectively. For numerical validation (see Table 3), 700 sample points have been manually classified using the aerial image (the total number of classified points was 5934). The rows are the classes of the manual classification, the columns are the classes of the SOM-based classification. The percentages in the diagonal show the the percentages of the waveforms that have been correctly classified (84.9% of the waveforms). The most significant case of misclassification is 8.8% of the waveforms, which has manually been classified as trees, was classified as grass in the SOM-based approach. This can possibly relate to seasonal changes.

	Grass	Roof	Tree	Pavement
Grass	21.6%	0.0%	0.4%	0.7%
Roof	0.3%	25.6%	0.3%	0.1%
Tree	8.8%	0.4%	4.2%	0.0%
Pavement	1.9%	0.0%	2.2%	33.5%

Table 3: Numerical verification of the classification process.

4 INFLUENCE OF THE COMPRESSION ON THE LAND CLASSIFICATION QUALITY

Table 4 summarizes effect of the compression on the classification. The rows show the original categories, the columns show the categories after decompression. The numbers in the diagonal

are the numbers of the waveforms whose classification did not change, the off-diagonal elements are the numbers of the misclassified waveforms.

The classification of 9.7% of the waveforms was affected by the compression method, while the classification of 90.3% of the waveforms did not change. The three significant cases were 2.4% of the tree waveforms being recognized as grass, 1.4% of the tree waveforms recognized as pavement, and 1.2% of the roof waveforms being recognized as pavement.

	Grass	Roof	Tree	Pavement
Grass	32.4%	0.0%	0.3%	0.2%
Roof	0.9%	18.3%	0.4%	1.2%
Tree	2.4%	0.1%	4.7%	1.4%
Pavement	1.0%	0.4%	1.4%	34.8%

Table 4: Effect of the compression on the classification

On the search for the cause of these significant misclassification cases, it was discovered, that depending on the shape of the original waveform, the estimation of ranges (used for the separation of roofs from pavement) was suffering from a high degree of degradation in some cases. Also some compression artifacts can affect the shape of the waveforms, thus altering its statistical parameters, and disturbing the peak detection method. These problems can be eliminated by further development of the compression algorithm.

5 THE ROLE OF THE COMPRESSION RATE

As stated before, the wavelet based compression has the advantage, that the user can choose between good compression ratio and low reconstruction error. Lowering the quantization threshold is expected to cause some loss in the compression performance, but is also expected to provide better reconstruction error statistics, thus increasing the performance of land classification. Also the fine tuning of the quantizer (e.g. using a non-linear quantization scheme) is to be carried out.

Quantization threshold	Misclassification percentage
1.0	8.0%
3.0	8.2%
5.0	9.7%
7.0	13.6%
9.0	15.1%

Table 5: The effect of compression on the classification performance using different quantization thresholds

The results of the initial experiments concerning the effect of the quantization threshold on the misclassification percentage can be seen in Table 5 (for the corresponding compression ratios and error statistics, see Table 2).

6 CONCLUSIONS

In this study we have developed a new methodology for an unsupervised classification of full-waveform LiDAR data, based on only the waveform shape parameters (i.e. no navigation data was used). We have also implemented an efficient method for the compression of the waveforms, in order to lower the storage and data transfer needs. The effect of the information loss caused by the lossy compression scheme on the classification quality was also studied.

For compression, the wavelet-based compression was used and the effectiveness of different wavelet families were examined. Finally, the biorthogonal CDF 3/9 was chosen with the best compression rates for this problem. The wavelet coefficients were thresholded first (with a value of 5.0) to discard the small coefficients representing unimportant features, and then a uniform mid-tread quantizer with 255 levels and RLE was applied to the data. With this method a compression rate of 0.21 was achieved, i.e. the data was compressed to less then one quarter of the original size, with the reconstruction error having a standard deviation of only 1 intensity value.

Both the original and the reconstructed waveform data was classified using an unsupervised classification method, the based on the SOM algorithm, and the efficiency of the waveform data to use for classification purposes was examined before and after compression.

Correlation was observed between the shape of the waveforms and the backscattering material. After the waveforms were separated into one- and multiple-echo waveforms, statistical parameters of the one-echo waveforms were calculated for the SOM-based classification (standard deviation, skewness, kurtosis and amplitude). As a result, the observation set was divided into three subsets, corresponding to trees, grass and non-vegetation areas. The classification was enhanced by separating the non-vegetation areas into pavement and roof, using the local range differences, calculated from the center of mass values and the starting time of the backscattered waveforms.

Visual comparison of the result of the classification with aerial imagery shows, that full-waveform LiDAR data can be used very efficiently to separate the different types of surfaces. Numerical verification shows a success rate of 84.9%.

Comparing the classification of the original and the reconstructed waveforms, 9.7% misclassification was observed. Further development of the compression and the classification algorithm is expected to overcome this difficulty.

ACKNOWLEDGMENTS

REFERENCES

Brattberg, O. and Tolt, G., 2008. Terrain classification using airborne lidar data and aerial imagery. The International Archives of the Photogrammetry, Remote Sensing and Spatial Information Sciences XXXVII(B3b), pp. 261–266.

Buckheit, J. B. and Donoho, D. L., 1995. Wavelab and reproducible research. Wavelets and Statistics, Springer-Verlag.

Chauve, A., Mallet, C., Bretar, F., Durrieu, S., Pierrot-Deseilligny, M. and Puech, W., 2007. Processing full-waveform lidar data: Modelling raw signals. International Archives of Photogrammetry, Remote Sensing and Spatial Information Sciences XXXVI(3/W52), pp. 102–107.

Cohen, A., Daubechies, I. and Feauveau, J.-C., 1992. Biorthogonal bases of compactly supported wavelets. Communications on Pure and Applied Mathematics 45(5), pp. 485 – 560.

Ducic, V., Hollaus, M., Ullrich, A., Wagner, W. and Melzer, T., 2006. 3d vegetation mapping and classification using full-waveform laser scanning. In: Proc. Workshop on 3D Remote Sensing in Forestry. EARSeL/ISPRS pp. 211–217.

Jutzi, B. and Stilla, U., 2005. Measuring and processing the waveform of laser pulses. In: A. Gruen and H. Kahmen (eds), Optical 3-D Measurement Techniques VII., Vol. I, pp. 194 – 203.

Kohonen, T., 1990. The self-organizing map. Proc. IEEE 78(9), pp. 1464–1480.

Kohonen, T., Hynninen, J., Kangas, J. and Laaksonen, J., 1996. Som_pak, the self-organizing map program package. Technical Report A31, Helsinki University of Technology, Laboratory of Computer and Information Science, FIN-02150 Espoo, Finland, 27 pages.

Laky, S., Zaletnyik, P. and Toth, C., 2010. Compressing LiDAR waveform data. Proceedings of the International LiDAR Mapping Forum 2010.

Maas, H. G., 1999. Fast determination of parametric house models from dense airborne laserscanner data. The International Archives of the Photogrammetry, Remote Sensing and Spatial Information Sciences XXXII(2/W1), pp. 1–6.

Mallet, C. and Bretar, F., 2009. Full-waveform topographic LiDAR: State-of-the-art. ISPRS Journal of Photogrammetry and Remote Sensing 64(1), pp. 1–16.

Mallet, C., Soergel, U. and Bretar, F., 2008. Analysis of full-waveform LiDAR data for an accurate classification of urban areas. International Archives of Photogrammetry, Remote Sensing and Spatial Information Sciences 37(Part 3A), pp. 85–92.

Sayood, K., 2006. Introduction to Data Compression. 3rd edn, (Morgan Kaufmann Series in Multimedia Information and Systems), Elsevier, San Francisco.

Shan, J. and Toth, C. K., 2009. Topographic laser ranging and scanning – principles and processing. CRC Press Taylor & Francis, London, 590 pages.

Wagner, W., Ullrich, A., Ducic, V., Melzer, T. and Studnicka, N., 2006. Gaussian decomposition and calibration of a novel small-footprint full-waveform digitising airborne laser scanner. ISPRS Journal of Photogrammetry and Remote Sensing 60(2), pp. 100 – 112.

Wagner, W., Ullrich, A., Melzer, T., Briese, C. and Kraus, K., 2004. From single pulse to full-waveform airborne laser scanners: Potential and practical challenges. International Archives of Photogrammetry, Remote Sensing and Spatial Information Sciences 35(Part B3), pp. 201 – 206.

Zaletnyik, P., Laky, S. and Toth, C., 2010. LiDAR waveform classification using self-organizing map. Proceedings of the ASPRS 2010 Annual Conference: Opportunities for Emerging Geospatial Technologies.